



Published in final edited form as:

J Infect Dis. 2017 September 15; 216(Suppl 4): S566–S574. doi:10.1093/infdis/jiw625.

Drug Susceptibility Evaluation of an Influenza A(H7N9) Virus by Analyzing Recombinant Neuraminidase Proteins

Larisa V. Gubareva¹, Katrina Sleeman^{1,a,b}, Zhu Guo^{1,a}, Hua Yang¹, Erin Hodges^{1,2}, Charles T. Davis¹, Tatiana Baranovich^{1,2}, James Stevens¹

¹Influenza Division, National Center for Immunization and Respiratory Diseases, Centers for Disease Control and Prevention,

²Carter Consulting, Atlanta, Georgia

Abstract

Background.—Neuraminidase (NA) inhibitors are the recommended antiviral medications for influenza treatment. However, their therapeutic efficacy can be compromised by NA changes that emerge naturally and/or following antiviral treatment. Knowledge of which molecular changes confer drug resistance of influenza A(H7N9) viruses (group 2NA) remains sparse.

Methods.—Fourteen amino acid substitutions were introduced into the NA of A/Shanghai/2/2013(H7N9). Recombinant N9 (recN9) proteins were expressed in a baculovirus system in insect cells and tested using the Centers for Disease Control and Prevention standardized NA inhibition (NI) assay with oseltamivir, zanamivir, peramivir, and laninamivir. The wild-type N9 crystal structure was determined in complex with oseltamivir, zanamivir, or sialic acid, and structural analysis was performed.

Results.—All substitutions conferred either reduced or highly reduced inhibition by at least 1 NA inhibitor; half of them caused reduced inhibition or highly reduced inhibition by all NA inhibitors. R292K conferred the highest increase in oseltamivir half-maximal inhibitory concentration (IC₅₀), and E119D conferred the highest zanamivir IC₅₀. Unlike N2 (another group 2NA), H274Y conferred highly reduced inhibition by oseltamivir. Additionally, R152K, a naturally occurring variation at the NA catalytic residue of A(H7N9) viruses, conferred reduced inhibition by laninamivir.

Conclusions.—The recNA method is a valuable tool for assessing the effect of NA changes on drug susceptibility of emerging influenza viruses.

Correspondence: L. V. Gubareva, Influenza Division, National Center for Immunization and Respiratory Diseases, Centers for Disease Control and Prevention, 1600 Clifton Road NE, MS-G16, Atlanta, GA, 30329 (LGubareva@cdc.gov).

^bPresent affiliation: Division of Global HIV/AIDS, Center for Global Health, Centers for Disease Control and Prevention, Atlanta, Georgia.

^aK. S. and Z. G. contributed equally to this study.

Publisher's Disclaimer: *Disclaimer.* The findings and conclusions of this report are those of the authors and do not necessarily represent the views of the funding agency, the Centers for Disease Control and Prevention.

Supplement sponsorship. This work is part of a supplement sponsored by the Centers for Disease Control and Prevention.

Potential conflicts of interest. All authors: No reported conflicts. All authors have submitted the ICMJE Form for Disclosure of Potential Conflicts of Interest. Conflicts that the editors consider relevant to the content of the manuscript have been disclosed.

Keywords

Neuraminidase; drug resistance; recombinant protein; A(H7N9); bird flu

Since 2013, avian influenza A(H7N9) viruses have been responsible for >800 human infections, mainly in China [1, 2]. These viruses cause asymptomatic infections in poultry, impeding their detection and measures to control virus spread [3]. Because of their persistence in avian populations, A(H7N9) viruses are likely to continue to inflict sporadic infections in humans, increasing the possibility for virus adaptation [4]. Unlike in avian species, A(H7N9) virus infections in humans have been associated with significant morbidity and mortality [4]. Local clusters of human infections have been detected, demonstrating that limited human-to-human transmission has occurred [5]. In addition, exported cases of A(H7N9) virus were detected in Malaysia, Taiwan, and North America, highlighting the public health concern over global spread of this dangerous respiratory pathogen [6–8].

Antivirals can alleviate the influenza burden and have been used successfully to treat patients infected with seasonal and zoonotic influenza viruses. Sequence analysis of the A(H7N9) genome revealed the presence of S31N in the M2 protein, an amino acid substitution that confers cross-resistance to adamantanes [1]. Neuraminidase (NA) inhibitors are the antivirals of choice for the treatment of A(H7N9) infections [9]. In the United States, oral oseltamivir and inhaled zanamivir were approved by the Food and Drug Administration in 1999; a third NA inhibitor, intravenous peramivir, was approved in December 2014. These 3 antivirals are also marketed in several other countries, including China. A fourth NA inhibitor, inhaled long-acting laninamivir, is currently licensed in Japan. Resistance to NA inhibitors is uncommon among currently circulating seasonal and zoonotic influenza viruses. However, emergence and rapid global spread of oseltamivir-resistant seasonal A(H1N1) viruses in 2008–2009 highlighted the alarming ability of drug-resistant influenza viruses to become transmissible and gain this selective advantage [10].

Understanding the mechanisms by which viruses become resistant to NA inhibitors is essential for effective virological surveillance and for making informed decisions with regard to clinical care. The key function of the influenza virus NA is to enhance virus mobility (spread) within the infected host. NA prevents entrapment of virus particles in mucin-rich secretions of the respiratory tract, averts aggregation of progeny virions, and facilitates egress from infected cells [11–13]. This is achieved via removal of neuraminic (sialic) acid residues from host receptors recognized by the viral hemagglutinin. By inhibiting NA enzyme activity, these drugs hamper the ability of influenza virus to multiply in the infected host. Structurally, NA inhibitors resemble the natural substrate neuraminic acid when it is bound to the enzyme's active site in a half-chair conformation [14, 15]. These drugs were rationally designed to produce tight interactions with conserved amino acid residues forming the NA active site. Conserved residues of the NA enzyme active site are divided into functional residues that make contact with the neuraminic acid and residues that provide required framework for catalysis [16].

Treatment of patients with oseltamivir and zanamivir has been shown to lead to the emergence of resistant viruses [17]. Prolonged treatment, immunocompromised status, and other factors are known to increase the risk for the emergence of resistance. Resistant viruses typically acquire an amino acid substitution in the NA that weakens drug binding. To detect potentially resistant viruses, a biochemical NA inhibition (NI) assay is used by surveillance laboratories. In this assay, a drug concentration needed to inhibit NA activity by 50% (IC₅₀) is determined and compared with a reference IC₅₀. Fold increases of <10, 10–100, and >100 are interpreted as normal, reduced inhibition (RI), or highly reduced inhibition (HRI) by a particular antiviral drug [18]. Although laboratory criteria for clinically relevant resistance to NA inhibitors have not yet been established, detection of HRI is often regarded as a sign of potential clinically relevant resistance. The list of NA changes found in seasonal viruses exhibiting RI/HRI is growing and undergoes regular revisions [19]. For convenience, all NA substitutions are described according to the N2 NA numbering scheme [16].

Because of subtle differences in the structure of NA proteins, a NA substitution that causes HRI in one subtype may not do so in another. For example, H274Y causes HRI by oseltamivir in N1 subtype viruses but not in the N2 subtype [20]. Moreover, structural similarities among NA inhibitors may result in cross-resistance among different drugs; for instance, H274Y in N1 confers HRI by both oseltamivir and peramivir. Expectedly, less information is available for newer NA inhibitors and emerging viruses.

A(H7N9) viruses collected from patients following oseltamivir treatment have been shown to develop changes in the NA that seem to confer resistance to oseltamivir and other NA inhibitors [1, 21–25]. Specifically, R292K was detected in A(H7N9) viruses recovered from humans [1, 21]. Emergence of E119V was also associated with oseltamivir treatment of patients infected with A(H7N9) viruses [25]. Notably, clonal analysis of an A(H7N9) virus recovered from an oseltamivir-treated patient in Taiwan revealed 4 distinct substitutions, R292K, E119V, I222R, and I222K [22]. Besides the clinical setting, the aptitude of A(H7N9) virus to quickly acquire NA changes conferring RI/HRI was demonstrated in nonhuman primates, whereby variant viruses were isolated from 3 of 6 animals treated with oseltamivir or peramivir [26]. Another concern is the unknown effects of natural variance observed among NA sequences in circulating A(H7N9) viruses [27].

Following the report on the detection of R292K in A/Shanghai/1/2013(H7N9), collected from the first documented infection in a human, we used recombinant protein technology to elucidate the effect of this change on the virus drug susceptibility, using 2 NA backbones, A/Shanghai/1/2013 and A/Anhui/2013 [23]. This approach offers a convenient and safe means to assess the effect of individual NA changes on drug susceptibility, especially when viruses are not available for testing. The ongoing threat posed by A(H7N9) to the human population prompted us to gain further insights into the molecular mechanisms of resistance and cross-resistance to the NA inhibitor class of anti-influenza drugs. In the present study, we extended our analysis by using a codon-optimized complementary DNA (cDNA) expressing recombinant N9 NA protein of A/Shanghai/2/2013(H7N9) and by introducing a series of NA amino acid substitutions that are known to confer RI/HRI in various NA subtypes. To aid in the analysis of the resulting NA inhibition profiles, crystal structures of the recombinant

N9 (recN9) proteins bound to the sialic acid and 2 NA inhibitors, oseltamivir and zanamivir, were determined, and structural analysis was performed.

MATERIALS AND METHODS

Recombinant NA Expression for the NI Assay and NA Activity Studies

A codon-optimized cDNA encoding residues 78–465 of the A(H7N9) NA gene of A/Shanghai/2/2013 (GISAID accession number EPI439500) was synthesized (GenScript) and subcloned into a pIEx-4 vector (EMD Millipore), using the In-Fusion HD cloning system (Clontech). recNA contained a His tag at the N-terminus followed by a tetramerization domain from human vasodilator-stimulated phosphoprotein [28] and a thrombin site [29]. All subsequent NA mutants were generated from this wild-type pIEx-4-NA clone, using the QuickChange Lightning Site-Directed Mutagenesis kit (Agilent). Resulting constructs were transiently transfected into Sf9 cells (EMD Millipore), using Cellfectin II transfection reagent (Invitrogen, ThermoFisher). Transfected cells were transferred into tissue culture flasks and grown on a shaker at 27°C for 5 days. The recNA secreted in the culture supernatant was quantified by Western blot detection of the His tag, using purified NA of A/Perth/16/2009(H3N2) as a standard. Supernatants were assessed for functional activity, using the 2'-(4-methylumbelliferyl)- α -D-N-acetylneuraminic acid assay and analyzed without further purification by means of the NI assay described below.

NA Inhibitors

The NA inhibitors oseltamivir carboxylate (oseltamivir; Hoffman-La Roche), zanamivir (GlaxoSmithKline), peramivir (BioCryst Pharmaceuticals), and R-125489 (laninamivir; Biota) were prepared in sterile distilled water and stored in aliquots at –30°C until use.

NI Assay

Inhibition of recNA enzyme activity of the 4 NA inhibitors was assessed in the fluorescence-based NA inhibition assay, using the NA-Fluor Influenza Neuraminidase Assay kit (Applied Biosystems, ThermoFisher) as previously described [30]. IC₅₀ values, defined as the concentration of drug required to reduce enzyme activity by 50%, were calculated using JASPR v1.2 curve-fitting software [30]. IC₅₀ values reported are the mean (\pm SD) of IC₅₀ values measured at least 3 times.

Recombinant NA Expression for Crystallization Studies

The codon-optimized NA gene of A/Shanghai/2/2013(H7N9) containing a His tag tetramerization domain and thrombin cleavage site as described above was also subcloned into the baculovirus transfer vector pAcGP67-B (BD Biosciences) for insect cell expression. Secreted proteins were recovered from the culture supernatant and purified by metal affinity chromatography and size exclusion chromatography. For structural analyses, the proteins were further subjected to trypsin cleavage and size exclusion chromatography. Trypsin-treated NA was buffer exchanged into 10 mM Tris-HCl, 50 mM NaCl, and 1 mM CaCl₂ (pH 8.0) and was concentrated to 4 mg/mL for crystallization trials.

Crystallization, Data Collection, Structure Determination, and Refinement

Initial crystallization trials were set up using a Topaz free-interface diffusion crystallizer system (Fluidigm). Diffraction quality crystals for NA were obtained at 20°C, using a modified method for micro-batch under oil [31]; the crystallization condition was 0.1 M HEPES:NaOH (pH 7.5) and 25% PEG 1000. Crystals of the NA/oseltamivir, NA/zanamivir, and NA/sialic acid complexes were obtained by soaking in 20 mM compound for 3 hours. Crystals were flash cooled at 100 K. Data were collected at the Advanced Photon Source beamline 22-ID at 100 K and processed with the DENZO-SACLEPACK suite [32]. Variables for which data were collected are presented in Table 1.

N9 NA structures were determined by molecular replacement with Phaser [33], using the A/Hangzhou/2/2013(H7N9) NA structure (Protein Data Bank identifier 4MWJ) as a search model. One NA monomer occupied the asymmetric unit, with an estimated solvent content of 60.4%, based on a Matthews coefficient (V_m) of 3.11 Å³/Da. The model was built by Coot [34], and then the protein structures were refined with REFMAC [35], using TLS refinement [36] and Phenix refine [37]. The 3 complexed NA structures were refined using the same strategy as for the apo NA structure. All final models were assessed using MolProbity [38], and statistics for data processing and refinement are presented in Table 1.

Protein Data Bank Accession Codes

The atomic coordinates and structure factors of N9 NA (apo and in complex with oseltamivir, zanamivir, and sialic acid) are available from the Protein Data Bank under accession codes 5L14, 5L15, 5L17, and 5L18.

RESULTS

Generation of Recombinant Influenza Virus N9 NA Proteins

In this study, 14 amino acid substitutions, which were reported to confer RI or HRI by NA inhibitor(s) in certain subtypes, were introduced into the codon-optimized cDNA encoding the NA of A/Shanghai/2/2013 (Table 2). This included 4 substitutions at the functional residues R152, E276, R292, and R371; 8 at the framework residues E119, I222, H274, and N294; within the NA active site and 2 residues, Q136 and T247, located in its proximity. In each instance, a single nucleotide change conferred the required amino acid substitution. The presence of the intended changes was confirmed by sequencing analysis of generated plasmids. The recN9 proteins were expressed in a transient expression system in Sf9 insect cells. All generated recN9 proteins were of expected size, determined by Western blot, and had NA activity (data not shown) sufficient for NI assay testing.

Assessment of Drug Susceptibility, Using the NI Assay

Experimental conditions (eg, buffer system, pH, and incubation time) have previously been shown to affect IC₅₀ values determined using NA inhibition assays. Therefore, the CDC standardized NI assay [30] was used to investigate the effect of the introduced amino acid substitutions on drug susceptibility. The resulting NA inhibition profiles for oseltamivir, zanamivir, peramivir, and laninamivir are shown in Table 3. In the A/Shanghai/2/2013 NA background, all changes yielded either RI or HRI by at least 1 NA inhibitor. The results

were grouped into 6 categories. In the first category, 5 substitutions, R152K, I222K, T247P, N294S, and R371K, conferred RI by 1 NA inhibitors. Notably, 2 of these, R371K at the functional residue and I222K at the framework, conferred RI by all 4 NA inhibitors. In the second, 3 substitutions, E119V, I222R, and H274Y, conferred HRI by oseltamivir. In addition, I222R conferred RI by the other 3 antiviral drugs. In the third, substitution R292K at the functional residue conferred HRI by oseltamivir and peramivir and RI by the other 2 NA inhibitors (Table 3). In the fourth, 2 substitutions, E276D at the functional residue and E119A at the framework, conferred HRI by zanamivir and also caused RI by the other 2 antiviral drugs. In the fifth, substitution E119G conferred HRI by zanamivir and laninamivir and RI by peramivir. In the sixth, 2 substitutions, E119D and Q136K, conferred HRI by the antiviral drugs, zanamivir, peramivir, and laninamivir. Additionally, E119D conferred RI by oseltamivir.

Structure of N9 NA

To understand the structural basis of the inhibition profiles, we solved the X-ray crystal structure of A/Shanghai/2/2013 recN9 protein; avian N9 NA numbering was used to describe the crystal structure findings. The structure was built and refined in I_{432} space group at a resolution of 1.9 Å. The final model that was generated included residues 83–470 (residues 82–468 in N2). The N9 NA structure is a typical box-shaped tetrameric association of identical monomers, containing six 4-stranded, antiparallel β -sheets that form a propeller-like arrangement (Figure 1A), as previously described for influenza A virus subtypes N1, N2, N4, N5, N8, and N9 and influenza B virus NA [14, 39–43]. One calcium ion-binding site, which is conserved in all known influenza A and influenza B virus NA proteins, was observed in N9 NA (Figure 1A). Ca^{2+} is bound through interactions with 2 water molecules and 4 backbone carbonyl oxygen atoms from N295, G299, D326, and N348 (residues 293, 297, 324, and 347 in N2). Ca^{2+} has been shown to be critical for the thermostability and activity of influenza virus NAs [44], and this conserved metal site was proposed to be important in stabilizing a reactive conformation of the active site by otherwise flexible loops [45]. Although N9 NA has 3 potential N-linked glycosylation sites, at N86, N147, and N202 (residues 85, 146, and 200 in N2), the final model had interpretable glycan density only at the 147 and 202 sites. N146 is situated on the membrane-distal surface close to the active site and is the only glycosylation site conserved among all other influenza A and B virus NAs [14, 39].

Among all of the subtypes, the enzyme-active site includes 8 highly conserved residues, R119, D152, R153, R226, E278, R294, R372, and Y406 (residues 118, 151, 152, 224, 276, 292, 371, and 406 in N2; Figure 1A). These are all charged/polar residues that directly interact with the substrate in the catalytic site. The geometry of the catalytic site is structurally stabilized through a network of hydrogen bonds and salt bridges by a constellation of largely conserved framework residues, E120, R157, W180, S181, N200, I224, E229, H276, E279, N296, and E425 (residues 119, 156, 178, 179, 198, 222, 227, 274, 277, 294, and 427 in N2) [42].

Next, we solved the crystal structures of N9 NA in complex with oseltamivir, zanamivir, and natural substrate, sialic (neuraminic) acid. Overall, the interactions between N9 NA and

inhibitors are similar (Figure 1B–D), although more hydrogen bonds are formed between NA and zanamivir. The carboxyl group of inhibitors hydrogen bonds to R119, R294, and R372 (residues 118, 292, and 371 in N2), while the carbonyl oxygen of the N-acetyl group hydrogen bonds with R153 (residue 152 in N2). The bulky 4-guanidino group of zanamivir is buried underneath the 150-loop and hydrogen bonds to D152, W180, and E229 (residues 151, 178, and 227 in N2). There are 2 additional hydrogen bond interactions between the zanamivir 8-hydroxyl group and R294 (residue 292 in N2) and 9-oseltamivir with R226 (residue 224 in N2) in the NA/zanamivir complex structure. E120 and I224 (residues 119 and 222 in N2) have hydrophobic interactions with the inhibitors. H275 (residue 274 in N2) does not have direct interactions with the inhibitors, but amino acid substitution at this location may cause the conformational change of E278 (residue 276 in N2) and the residues on 240-loop, which are involved in binding of inhibitors. Q137K (residue 136 in N2) also does not interact directly with the inhibitors; however, this substitution can adversely affect the binding of the guanidyl group of zanamivir by interfering with the hydrogen bond formation between residue 137 and the main chain carbonyl of D152 (residue 151 in N2) on 150-loop.

DISCUSSION

Through the NA inhibition analysis of recN9 proteins carrying one of 14 designated amino acid substitutions, we provided further insights into molecular markers that can alter drug susceptibility of avian influenza A(H7N9) viruses. The recNA protein approach offers a convenient means to study effects of NA changes, identified in field isolates or viruses recovered from drug-treated patients, on drug susceptibility. Notably, this experimental approach enables the drug phenotype to be determined without a need to work directly with live virus. Our data provide the experimental evidence for N9 subtype-specific profiles of resistance to the NA inhibitors.

Based on a phylogenetic analysis, N9 belongs to group 2 NA, shared by N2, N3, N6, and N7 subtypes [39]. The phylogenetic and structural similarities among this group explain why 2 substitutions, E119V and R292K, are the most reported changes in viruses of N2 and N9 subtypes, including A(H7N9) virus, that are linked to drug resistance. The H274Y is the marker of oseltamivir resistance in N1 (group 1NA) but not in N2 [20]. Therefore, we decided to introduce this change into recN9 to substantiate the suspected similarities between the N2 and N9 subtypes. If confirmed, such a finding would simplify drug phenotype predictions for the emerging A(H7N9) virus because much more information is available on seasonal A(H3N2) viruses. Unexpectedly, H274Y in recN9 of A/Shanghai/2/2013 conferred HRI (105-fold) by oseltamivir and also increased peramivir IC₅₀ values by 9-fold. Our results are in agreement with those of Song et al, where H274Y in NA of A/duck/Memphis/546/1974(H11N9) conferred a 90-fold increase in oseltamivir IC₅₀ and an 11-fold increase in peramivir IC₅₀ [46]. In the NA of A/Shanghai/2/2013, H274Y requires a C→U substitution at the first nucleotide of the triplet encoding histidine; similarly, Q136K requires a C→A substitution at the first codon, as well. Notably, the random mutagenesis approach, coupled with passaging of virus in the presence of zanamivir, led to the emergence of Q136K (CAA→AAA) in N9 of A/duck/Memphis/546/1974 [46]. They also reported selection of A246T; this change conferred 25- and 6-fold increases in

zanamivir and oseltamivir IC_{50} values, respectively. In our study, substitution introduced at a neighboring residue, T247P, conferred 69- and 27-fold increases in zanamivir and oseltamivir IC_{50} values, respectively. This change was introduced in recN9 because our previous finding showed that RI by both zanamivir (66-fold) and oseltamivir (31-fold) in A(H3N2) virus was linked to a mutation at this position [47]. The proline that replaced threonine at position 247 is likely to provide more rigidity to the 240–amino acid loop affecting the flexibility and positioning of this loop and its contribution in the hydrogen bonding network involved in NA inhibitor binding.

In the present study, all amino acid substitutions introduced into the recN9 have conferred either RI or HRI by at least 1 antiviral drug. Seven substitutions caused RI/HRI to all antiviral drugs tested; 3 were made at catalytic residues (E276, R292, and R371). Conversely, R152K, a substitution at another catalytic residue, conferred RI by laninamivir only. R292K and E119D substitutions not only conferred RI or HRI by all 4 NA inhibitors, but also caused the highest increases in IC_{50} values.

The susceptibility profiles for I222R and I222K in recN9 were similar to those determined for clones of A/Taiwan/1/2013(H7N9), validating the recombinant protein approach for characterization of emerging influenza viruses. The emergence of another substitution, I222T, was detected in a nonhuman primate infected with A/Anhui/1/2013(H7N9) treated with oseltamivir [26]. I222M was reported in recombinant PR8 virus carrying N9 (A/duck/Memphis/546/1974) when it was propagated in the presence of oseltamivir. All 4 substitutions—I222R/K/T/M—caused RI by oseltamivir (143-, 46-, 20-, and 18-fold, respectively) in the N9 subtype.

It is worth noting that inhibition profiles obtained using the CDC standardized NI assay with the 4 NA inhibitors can be used to predict the NA change. For example, if 2009 pandemic influenza A(H1N1) virus exhibits HRI by oseltamivir (approximately 800-fold) and peramivir (approximately 350-fold) while showing normal inhibition by zanamivir and laninamivir, such a virus predictably harbors H275Y. The use of the standardized assay also offers advantages by simplifying interpretation and improving exchange of information between surveillance laboratories.

Sequence-based monitoring of drug resistance has become common with the improvement of sequencing methods. While summarizing this study's results, we queried the public database (GISAID) and found substitutions E119V ($n = 5$), R152K ($n = 3$), I222K ($n = 1$), I222R ($n = 1$), and R292K ($n = 13$) among 1177 available NA sequences of N9 subtype (Table 4). Two factors are likely to contribute to the low detection rate of known/potential markers: (1) consensus sequences are deposited into the database, which may mask the presence of drug resistant variants in a sample [22]; and (2) specimen collection is often done before initiating antiviral treatment. Another plausible explanation could be the adverse effects of drug resistance–conferring mutations on virus transmissibility and replicative fitness. Interpretation of laboratory data for making treatment decisions is complicated because of limited knowledge of drug resistance in clinical settings. In a ferret model, oseltamivir resistance was observed in animals experimentally infected with A(H7N9) viruses carrying either R292K or E119V; both viruses had HRI by oseltamivir

[22]. Notably, in animals infected with the virus carrying I222K, the therapeutic effect of oseltamivir was also diminished. This virus exhibited RI (32-fold) by oseltamivir [22]. Therefore, NA changes conferring RI need to be closely monitored. Additional studies are required to improve interpretation of the NI assay results and to establish laboratory correlates of clinically relevant resistance to all NA inhibitors.

Unusual NA changes can alter drug susceptibility (eg, T247P), as has been shown here and by others [46]. These findings advocate the need for empirical testing of viruses by use of the NI assay in addition to sequence analysis. The development of highly sensitive NA activity–based assays that can be performed on respiratory specimens will enhance surveillance and facilitate clinical care decisions in the future. Rapid replication and high loads of A(H7N9) viruses may contribute to the emergence of resistance. Virological surveillance is vital for detecting transmissible drug-resistant viruses. The recombinant NA protein technology provides a powerful tool for establishing markers that have a potential to cause drug resistance among emerging A(H7N9) viruses.

Acknowledgments.

We thank our colleagues Anton Chesnokov and Ha T. Nguyen (Battelle) and members of the Zoonotic Virus Team at the Influenza Division, Centers for Disease Control and Prevention, for valuable contributions to this project; and the manufacturers Roche, GSK, BioCryst, and Biota, who kindly provided neuraminidase inhibitors.

Financial support. This work was supported by the Centers for Disease Control and Prevention.

References

1. Gao R, Cao B, Hu Y, et al. Human infection with a novel avian-origin influenza A (H7N9) virus. *N Engl J Med* 2013; 368:1888–97. [PubMed: 23577628]
2. Lam TT, Zhou B, Wang J, et al. Dissemination, divergence and establishment of H7N9 influenza viruses in China. *Nature* 2015; 522:102–5. [PubMed: 25762140]
3. Pantin-Jackwood MJ, Miller PJ, Spackman E, et al. Role of poultry in the spread of novel H7N9 influenza virus in China. *J Virol* 2014; 88:5381–90. [PubMed: 24574407]
4. Zhu H, Lam TT, Smith DK, Guan Y. Emergence and development of H7N9 influenza viruses in China. *Curr Opin Virol* 2016; 16:106–13. [PubMed: 26922715]
5. Zhang Y, Shen Z, Ma C, et al. Cluster of human infections with avian influenza A (H7N9) cases: a temporal and spatial analysis. *Int J Environ Res Public Health* 2015; 12:816–28. [PubMed: 25599373]
6. William T, Thevarajah B, Lee SF, et al. Avian influenza (H7N9) virus infection in Chinese tourist in Malaysia, 2014. *Emerg Infect Dis* 2015; 21:142–5. [PubMed: 25531078]
7. Yang JR, Kuo CY, Huang HY, et al. Characterization of influenza A (H7N9) viruses isolated from human cases imported into Taiwan. *PLoS One* 2015; 10:e0119792. [PubMed: 25748033]
8. Skowronski DM, Chambers C, Gustafson R, et al. Avian Influenza A(H7N9) Virus Infection in 2 Travelers Returning from China to Canada, January 2015. *Emerg Infect Dis* 2016; 22:71–4. [PubMed: 26689320]
9. Centers for Disease Control and Prevention. Interim guidance on the use of antiviral agents for treatment of human infections with avian influenza A (H7N9) virus. <http://www.cdc.gov/flu/avianflu/h7n9-antiviral-treatment.htm>. Accessed July 28 2016.
10. Moscona A. Global transmission of oseltamivir-resistant influenza. *N Engl J Med* 2009; 360:953–6. [PubMed: 19258250]
11. Cohen M, Zhang XQ, Senaati HP, et al. Influenza A penetrates host mucus by cleaving sialic acids with neuraminidase. *Virol J* 2013; 10:321. [PubMed: 24261589]

12. Matrosovich MN, Matrosovich TY, Gray T, Roberts NA, Klenk HD. Neuraminidase is important for the initiation of influenza virus infection in human airway epithelium. *J Virol* 2004; 78:12665–7. [PubMed: 15507653]
13. Shtyrya YA, Mochalova LV, Bovin NV. Influenza virus neuraminidase: structure and function. *Acta Naturae* 2009; 1:26–32. [PubMed: 22649600]
14. Varghese JN, Epa VC, Colman PM. Three-dimensional structure of the complex of 4-guanidino-Neu5Ac2en and influenza virus neuraminidase. *Protein Sci* 1995; 4:1081–7. [PubMed: 7549872]
15. Collins PJ, Haire LF, Lin YP, et al. Structural basis for oseltamivir resistance of influenza viruses. *Vaccine* 2009; 27:6317–23. [PubMed: 19840667]
16. Colman PM, Hoynes PA, Lawrence MC. Sequence and structure alignment of paramyxovirus hemagglutinin-neuraminidase with influenza virus neuraminidase. *J Virol* 1993; 67:2972–80. [PubMed: 8497041]
17. Nguyen HT, Fry AM, Gubareva LV. Neuraminidase inhibitor resistance in influenza viruses and laboratory testing methods. *Antivir Ther* 2012; 17(1 Pt B):159–73. [PubMed: 22311680]
18. World Health Organization. Meetings of the WHO working group on surveillance of influenza antiviral susceptibility—Geneva, November 2011 and June 2012. *Wkly Epidemiol Rec* 2012; 87:369–74. [PubMed: 23061103]
19. World Health Organization. Laboratory methodologies for testing the antiviral susceptibility of influenza viruses. Summary of neuraminidase amino acid substitutions associated with reduced inhibition by neuraminidase inhibitors. http://www.who.int/influenza/gisrs_laboratory/antiviral_susceptibility/avwg2014_nai_substitution_table.pdf?ua=1. Accessed July 29 2016.
20. Abed Y, Baz M, Boivin G. Impact of neuraminidase mutations conferring influenza resistance to neuraminidase inhibitors in the N1 and N2 genetic backgrounds. *Antivir Ther* 2006; 11:971–6. [PubMed: 17302366]
21. Hu Y, Lu S, Song Z, et al. Association between adverse clinical outcome in human disease caused by novel influenza A H7N9 virus and sustained viral shedding and emergence of antiviral resistance. *Lancet* 2013; 381:2273–9. [PubMed: 23726392]
22. Marjuki H, Mishin VP, Chesnokov AP, et al. Characterization of drug-resistant influenza A(H7N9) variants isolated from an oseltamivir-treated patient in Taiwan. *J Infect Dis* 2015; 211:249–57. [PubMed: 25124927]
23. Sleeman K, Guo Z, Barnes J, Shaw M, Stevens J, Gubareva LV. R292K substitution and drug susceptibility of influenza A(H7N9) viruses. *Emerg Infect Dis* 2013; 19:1521–4. [PubMed: 23965618]
24. Yen HL, McKimm-Breschkin JL, Choy KT, et al. Resistance to neuraminidase inhibitors conferred by an R292K mutation in a human influenza virus H7N9 isolate can be masked by a mixed R/K viral population. *MBio* 2013; 4.
25. Mok CK, Chang SC, Chen GW, et al. Pyrosequencing reveals an oseltamivir-resistant marker in the quasispecies of avian influenza A (H7N9) virus. *J Microbiol Immunol Infect* 2015; 48:465–9. [PubMed: 24388586]
26. Itoh Y, Shichinohe S, Nakayama M, et al. Emergence of H7N9 Influenza A Virus Resistant to Neuraminidase Inhibitors in Nonhuman Primates. *Antimicrob Agents Chemother* 2015; 59:4962–73. [PubMed: 26055368]
27. Zaraket H, Baranovich T, Kaplan BS, et al. Mammalian adaptation of influenza A(H7N9) virus is limited by a narrow genetic bottleneck. *Nat Commun* 2015; 6:6553. [PubMed: 25850788]
28. Kühnel K, Jarchau T, Wolf E, et al. The VASP tetramerization domain is a righthanded coiled coil based on a 15-residue repeat. *Proc Natl Acad Sci U S A* 2004; 101:17027–32. [PubMed: 15569942]
29. Xu X, Zhu X, Dwek RA, Stevens J, Wilson IA. Structural characterization of the 1918 influenza virus H1N1 neuraminidase. *J Virol* 2008; 82:10493–501. [PubMed: 18715929]
30. Okomo-Adhiambo M, Mishin VP, Sleeman K, et al. Standardizing the influenza neuraminidase inhibition assay among United States public health laboratories conducting virological surveillance. *Antiviral Res* 2016; 128:28–35. [PubMed: 26808479]
31. Chayen NE, Stewart PDS, Blow DM. Microbatch crystallization under oil — a new technique allowing many small-volume crystallization trials. *Journal of Crystal Growth* 1992; 122:176–80.

32. Otwinowski Z, Minor W. Processing of X-ray Diffraction Data Collected in Oscillation Mode. In: Carter CW Jr, Sweet RM, eds. *Methods in enzymology*. Vol 276. Macromolecular crystallography, part A: Academic Press, 1997:307–26.
33. McCoy AJ, Grosse-Kunstleve RW, Storoni LC, Read RJ. Likelihood-enhanced fast translation functions. *Acta Crystallogr D Biol Crystallogr* 2005; 61(Pt 4):458–64. [PubMed: 15805601]
34. Emsley P, Cowtan K. Coot: model-building tools for molecular graphics. *Acta Crystallogr D Biol Crystallogr* 2004; 60(Pt 12 Pt 1):2126–32. [PubMed: 15572765]
35. Collaborative Computational Project N. The CCP4 suite: programs for protein crystallography. *Acta Crystallogr D Biol Crystallogr* 1994; 50:760–3. [PubMed: 15299374]
36. Winn MD, Isupov MN, Murshudov GN. Use of TLS parameters to model anisotropic displacements in macromolecular refinement. *Acta Crystallogr D Biol Crystallogr* 2001; 57(Pt 1):122–33. [PubMed: 11134934]
37. Adams PD, Afonine PV, Bunkóczi G, et al. PHENIX: a comprehensive Pythonbased system for macromolecular structure solution. *Acta Crystallogr D Biol Crystallogr* 2010; 66(Pt 2):213–21. [PubMed: 20124702]
38. Davis IW, Leaver-Fay A, Chen VB, et al. MolProbity: all-atom contacts and structure validation for proteins and nucleic acids. *Nucleic Acids Res* 2007; 35(Web Server issue):W375–83. [PubMed: 17452350]
39. Russell RJ, Haire LF, Stevens DJ, et al. The structure of H5N1 avian influenza neuraminidase suggests new opportunities for drug design. *Nature* 2006; 443:45–9. [PubMed: 16915235]
40. Baker AT, Varghese JN, Laver WG, Air GM, Colman PM. Three-dimensional structure of neuraminidase of subtype N9 from an avian influenza virus. *Proteins* 1987; 2:111–7. [PubMed: 3447170]
41. Wang M, Qi J, Liu Y, et al. Influenza A virus N5 neuraminidase has an extended 150-cavity. *J Virol* 2011; 85:8431–5. [PubMed: 21653672]
42. Burmeister WP, Ruigrok RW, Cusack S. The 2.2 Å resolution crystal structure of influenza B neuraminidase and its complex with sialic acid. *EMBO J* 1992; 11:49–56. [PubMed: 1740114]
43. Wu Y, Bi Y, Vavricka CJ, et al. Characterization of two distinct neuraminidases from avian-origin human-infecting H7N9 influenza viruses. *Cell Res* 2013; 23:1347–55. [PubMed: 24165891]
44. Burmeister WP, Cusack S, Ruigrok RW. Calcium is needed for the thermostability of influenza B virus neuraminidase. *J Gen Virol* 1994; 75 (Pt 2):381–8. [PubMed: 8113759]
45. Smith BJ, Huyton T, Joosten RP, et al. Structure of a calcium-deficient form of influenza virus neuraminidase: implications for substrate binding. *Acta Crystallogr D Biol Crystallogr* 2006; 62(Pt 9):947–52. [PubMed: 16929094]
46. Song MS, Marathe BM, Kumar G, et al. Unique Determinants of Neuraminidase Inhibitor Resistance among N3, N7, and N9 Avian Influenza Viruses. *J Virol* 2015; 89:10891–900. [PubMed: 26292325]
47. Sleeman K, Mishin VP, Guo Z, et al. Antiviral susceptibility of variant influenza A(H3N2)v viruses isolated in the United States from 2011 to 2013. *Antimicrob Agents Chemother* 2014; 58:2045–51. [PubMed: 24449767]

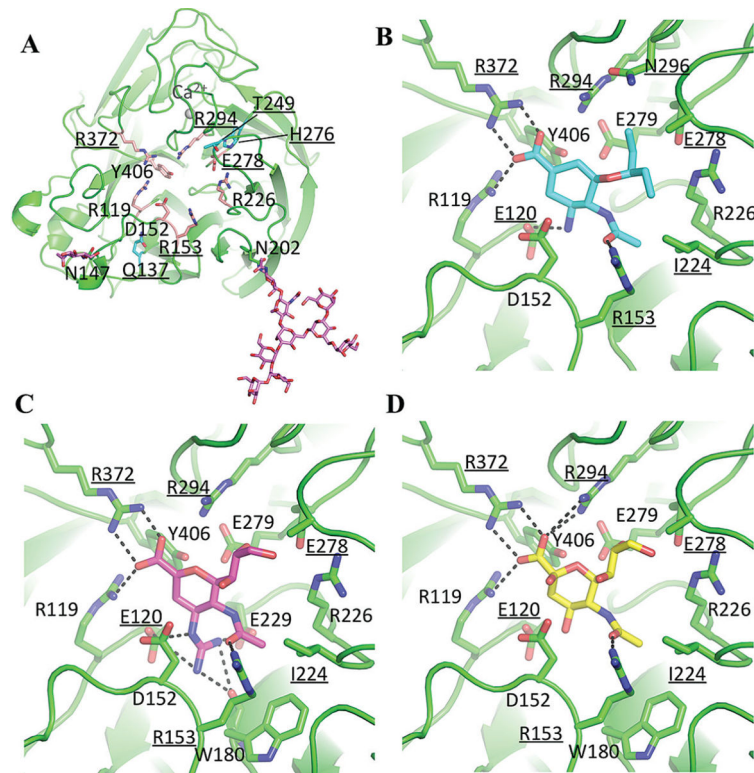


Figure 1.

The structures of N9 neuraminidase (NA) and its complexes (the avian N9 numbering scheme is used). The 10 residues that were substituted in this study are underlined (Table 2). *A*, Overall structure of the NA monomer, with highly conserved residues of the active site presented as salmon sticks. Residues Q137, T249, and H276 are shown as cyan sticks. Two occupied glycosylation sites are labeled, and glycans are shown as magenta sticks. *B*, The active site with oseltamivir. *C*, The active site with zanamivir. *D*, The active site with sialic (neuraminic) acid. The dashed lines are hydrogen bonds. The structural figure was generated with MacPyMol.

Table 1.

Data Collection and Refinement Statistics

	Variable			
	NA	NA/Ose	NA/Zan	NA/SA
General				
Space group	I432	I432	I432	I432
Cell dimension, Å	181.87	182.44	181.28	181.75
Cell angle, deg	90	90	90	90
Resolution, Å	50–1.9 (1.97–1.9)	50–2.4 (2.49–2.4)	50–2.4 (2.49–2.4)	50–1.8 (1.86–1.8)
R_{sym} or R_{merge} , %	0.081 (0.661)	0.101 (0.641)	0.095 (0.472)	0.137 (0.309)
I/σ	27.3 (2.4)	23.2 (2.3)	26.2 (3.3)	69.2 (16.6)
Completeness, %	99.3 (98.3)	97.6 (93.9)	94.7 (98.1)	100 (99.9)
Redundancy	6.5 (5.8)	7.5 (6.7)	5.3 (5.4)	13.6 (10.3)
Refinement				
Resolution, Å	35.7–1.9 (1.97–1.9)	40.8–2.4 (2.49–2.4)	38.7–2.4 (2.49–2.4)	40.6–1.8 (1.86–1.8)
Reflections, total no.	40 109	20 042	18 975	47423
Reflections, no. (test)	3921	1885	1943	4663
$R_{\text{work}}/R_{\text{free}}$, %	16.7/18.3	16.7/19.5	20.6/25.6	13.7/16.1
Atoms, no.	3607	3389	3416	3752
Root mean square deviation				
Bond length, Å	0.004	0.005	0.005	0.006
Bond angle, deg	0.86	0.92	0.94	1.07
MolProbity score				
Favored, %	95	96	95	96
Outliers, % (proportion)	0.77 (3/399)	0	0.26 (1/400)	0
PDB accession code	5L14	5L15	5L17	5L18

Abbreviations: Ose, oseltamivir; PDB, Protein Data Bank; SA, sialic acid; Zan, zanamivir.

Table 2.

Amino Acid Substitutions Introduced Into the Recombinant Neuraminidase (NA) Proteins of Influenza A/Shanghai/2/2013(H7N9) Virus

NA Residue ^a		Amino Acid ^b		Amino Acid Change	Function ^c	RI/HRIF ^e Reported in	Nucleotide Change in A/Shanghai/2/2013 NA
N2	Avian N9	N9 (H7N9)	Amino Acid				
119	120	115	E	A	FW	N1, N2, B	GAA → GCA
...	D	...	N1, N2, N7, B	GAA → GAU
...	G	...	N1, N2, N3, N7, N9, B	GAA → GGA
...	V	...	N1, N2, N7, N9, N9 (2013), B	GAA → GUA
136	137	132	Q	K	-	N1 ^f , N2, N9	CAA → AAA
152	153	148	R	K	Cat	B, N9	AGG → AAG
222	224	219	I	K	FW	N1, N9 (2013)	AUA → AAA
...	R	...	N1, N9 (2013)	AUA → AGA
247	249	244	S(T) ^g	P	-	N2 ^v	ACU → CCU
274	276	271	H	Y	FW	N1, N3, N9, B	CAU → UAU
276	278	273	E	D	Cat	N2, N7	GAA → GAC
292	294	289	R	K	Cat	N2, N3, N6, N7, N9, N9 (2013)	AGG → AAG
294	296	291	N	S	-	N1, N2, B	AAU → AGU
371	372	367	R	K	Cat	N2, B	AGG → AAG

Abbreviations: Cat, catalytic residue; FW, framework residue; -, nonactive site/unspecified.

^a Amino acid position in the NA that is known or suspected to adversely affect susceptibility to NA inhibitor(s). N2, avian N9, and 2013 N9-specific numbering schemes were used.^b Amino acid at the indicated residue of the NA gene of A/Victoria/361/2001(H3N2), A/Shanghai/2/2013(H7N9), and A/tern/Australia/G70C/1975(H11N9).^c The function of the NA residue is based on findings by Colman et al [16].^d Compared with the NA sequence of A/Shanghai/2/2013(H7N9) virus. The difference is shown in bold.^e Reduced (RI) or highly reduced inhibition (HRI) were determined using the NA inhibition assay. See also Table 4.^f Was shown to be host-cell selected.^g Serine is a highly conserved amino acid residue in A(H3N2) viruses, whereas tyrosine is predominant in avian N9 viruses.

Table 3. Inhibition Profiles of Recombinant Neuraminidase (NA) Proteins of Influenza A/Shanghai/2/2013(H7N9) Virus, Based on the Fluorescence-Based NA Inhibition Assay

NA Change (N2) or Group ^a	NA change (Avian N9)	IC ₅₀ , nM, Mean ± SD (Fold Change ^c)			
		Osetamivir	Zanamivir	Peramivir	Laminamivir
Normal inhibition					
None	None	0.27 ± 0.01 [1]	0.50 ± 0.05 [1]	0.07 ± 0.01 [1]	0.53 ± 0.03 [1]
Reduced or highly reduced inhibition					
Reduced inhibition by at least 1 NA inhibitor					
R152K	R153K	0.09 ± 0.01 [1]	2.71 ± 0.06 [5]	0.19 ± 0.01 [3]	8.40 ± 0.69 [16] ^d
I222K	I224K	12.48 ± 1.12 [46] ^d	8.32 ± 0.22 [17] ^d	0.80 ± 0.02 [11] ^d	14.32 ± 1.06 [27] ^d
T247P	T249P	7.34 ± 0.78 [27] ^d	34.60 ± 2.36 [69] ^d	0.30 ± 0.05 [4]	4.51 ± 0.33 [9]
N294S	N296S	0.54 ± 0.05 [2]	4.83 ± 0.45 [10] ^d	0.10 ± 0.01 [1]	1.35 ± 0.06 [3]
R371K	R372K	18.91 ± 13.0 [70] ^d	32.24 ± 2.55 [64] ^d	2.00 ± 0.21 [29] ^d	9.94 ± 0.95 [19] ^d
Highly reduced inhibition by oseltamivir					
E119V	E120V	45.64 ± 0.98 [169] ^d	4.42 ± 0.30 [9]	0.11 ± 0.01 [1]	0.86 ± 0.05 [2]
I222R	I224R	38.55 ± 3.61 [143] ^d	18.89 ± 2.02 [38] ^d	3.10 ± 0.13 [44] ^d	33.54 ± 1.70 [63] ^d
H274Y	H276Y	28.32 ± 2.30 [105] ^d	1.09 ± 0.08 [2]	0.66 ± 0.05 [9]	1.09 ± 0.08 [2]
Highly reduced inhibition by oseltamivir and peramivir					
R292K	R294K	>10 000 [>10 000] ^d	33.25 ± 2.65 [67] ^d	174.10 ± 8.38 [2487] ^d	16.40 ± 1.82 [31] ^d
Highly reduced inhibition by zanamivir					
E119A	E120A	5.01 ± 0.59 [19] ^d	114.12 ± 9.50 [228] ^d	1.43 ± 0.17 [20] ^d	32.8 ± 2.01 [62] ^d
E276D	E278D	3.64 ± 1.30 [13] ^d	213.52 ± 78.88 [427] ^d	1.74 ± 0.72 [25] ^d	47.51 ± 13.50 [90] ^d
Highly reduced inhibition by zanamivir and peramivir					
E119G	E120G	0.42 ± 0.07 [2]	209.54 ± 10.07 [419] ^d	3.35 ± 0.25 [48] ^d	65.93 ± 2.68 [124] ^d
Highly reduced inhibition by zanamivir, peramivir, and laminamivir					
E119D	E120D	3.77 ± 0.18 [14] ^d	718.14 ± 70.11 [1436] ^d	28.75 ± 3.43 [411] ^d	203.06 ± 38.68 [383] ^d

NA Change (N2) or Group ^a	NA change (Avian N9)	IC ₅₀ ^b , nM, Mean ± SD (Fold Change) ^c			
		Osetamivir	Zanamivir	Peramivir	Laninamivir
Q136K	Q137K	0.08 ± 0.01 [1]	350.91 ± 32.19 [702] ^d	9.19 ± 0.83 [131] ^d	166.12 ± 11.94 [313] ^d
Control A(H1N1)pdm09 viruses ^e					
None	None	0.18 ± 0.06	0.15 ± 0.03	0.04 ± 0.01	0.12 ± 0.01
H274Y	H276Y	149.72 ± 30.40 [812] ^d	0.18 ± 0.02 [1]	14.92 ± 1.89 [348] ^d	0.26 ± 0.02 [2]

Abbreviations: A(H1N1)pdm09, 2009 pandemic influenza A(H1N1) virus; IC₅₀, half-maximal inhibitory concentration; recN9, recombinant N9.

^a Amino acid numbering is based on the N2 and N9 numbering schemes. See also Table 2.

^b The IC₅₀ denotes the concentration of a NA inhibitor that reduces the NA activity of recNA9 by 50% relative to NA activity without the inhibitor. Values represents the average of at least 3 independent experiments.

^c Fold change relative to the mean IC₅₀ of the recN9 wild-type NA protein. Fold-change values of each recN9 were interpreted using criteria established by the World Health Organization Influenza Antiviral Working Group [18].

^d Fold change >10 (ie, reduced/highly reduced inhibition).

^e A/California/12/2012(H1N1)pdm09 wild-type (none) and A/Texas/23/2012(H1N1)pdm09 (H274Y).

Table 4.

Variations at Amino Acid Residues of Interest Among 1177 Complete-Length Neuraminidase (NA) Gene Sequences of Influenza A(H7N9) Viruses Available in the GISAID Database, 1 January 2013–25 July 2016

NA Residue		2013 N9	Amino Acid ^d	Amino Acid Change	Sequences With Amino Acid Change	No.	Accession Numbers (Passage History)
N2	Avian N9						
119	120	115	E ^b	V	5	EPIISL_141162 A/Jiangsu/02/2013 (E1); EPIISL_158942 A/Taiwan/01/2013 (E1/S2); EPIISL_192328 A/Anhui/01881/2014 (E1); EPIISL_192348 A/Zhejiang/16/2014 (E1); EPIISL_192354 A/Guangdong-Guangzhou/XN14670/2014 (E1) EPIISL_206852 Am/chicken/Huai'an/007/2014 (NR); EPIISL_206854 A/chicken/Huai'an/053/2014 (NR)	
152	153	148	R	K	3	EPIISL_141174 Am/Shanghai/9/2013 (E1); EPIISL_175722 A/silkie_chicken/Dongguan/3990/2013 (E1); EPIISL_192505 A/Zhejiang/9/2015 (E1) EPIISL_206853 A/Huai'an/062/2014 (NR) EPIISL_158944 A/Taiwan/01/2013 (E1/S2/NA/I222K) EPIISL_158943 A/Taiwan/01/2013 (E1/S2/NA/I222R)	
222	224	219	I	T	1	EPIISL_138737 A/Shanghai/1/2013 (E1); EPIISL_141186 A/Jiangsu/07/2013 (E1); EPIISL_141166 A/Shanghai/06-A/2013 (E1); EPIISL_142187 A/Taiwan/S02076/2013 (NR); EPIISL_155053 A/Taiwan/01/2013 (E1/S2/NA/R292K); EPIISL_155654 Am/Shanghai/5190Tm/2013 (NR); EPIISL_166435 Am/Zhejiang/LS01/2014 (NR); EPIISL_175835 A/Shenzhen/SP44/2014 (NR); EPIISL_190691 A/Quzhou/1/2015 (NR); EPIISL_192344 A/Zhejiang/22/2014 (E1); EPIISL_192371 A/Guangdong-Guangzhou/XN00429/2014 (E1); EPIISL_192377 A/Shandong/01/2014 (E1); EPIISL_192440 A/Zhejiang/07803/2014 (E1)	
292	294	289	R ^c	K	13		

Author Manuscript

Author Manuscript

Author Manuscript

Author Manuscript

The variations at the following amino acid positions were analyzed: 119, 136, 152, 222, 247, 274, 276, 292, 294, and 371 (N2 numbering), 2013 N9-specific numbering accounts for the amino acid residue deletion at positions 64–8.

Abbreviation: NR, not reported.

^aResidue in influenza A/Victoria/361/2001(H3N2), A/Anhui/1/2013(H7N9), and A/tern/Australia/G70C/1975(H11N9) viruses.

^bThree sequences have indeterminate (ie, “x”) nucleotide(s) within the triplet encoding amino acid residue 119.

^cTwo sequences have indeterminate (ie, “x”) nucleotide(s) within the triplet encoding amino acid residue 292.